Millennial-scale Vulnerability of the Antarctic Ice Sheet to Regional Ice Shelf Collapse

Daniel F. Martin[1], **Stephen L. Cornford** [2,3], **Antony J. Payne**[3]

[1]Computational Research Division, Lawrence Berkeley National Laboratory, Berkeley, CA, USA
[2]Department of Geography, College of Science, Swansea University, Swansea, UK
[3]Centre for Polar Observation and Modelling, School of Geographical Sciences, University of Bristol, Bristol, UK

Key Points:

- Sustained ice-shelf loss in any of the Amundsen Sea, Ronne, or Ross sectors can lead to wholesale West Antarctic ungrounding and collapse
- Even with extreme forcing, loss is relatively modest for the initial century, increasing markedly after in West Antarctic collapse scenarios.
- Modeling suggests Antarctic drainage basins can be assumed to be dynamically independent for 1-2 centuries before they begin to interact.

Corresponding author: D.F. Martin, `DFMartin@lbl.gov`

Abstract

The Antarctic Ice Sheet (AIS) remains the largest uncertainty in projections of future sea level rise. A likely climate-driven vulnerability of the AIS is thinning of floating ice shelves resulting from surface-melt-driven hydrofracture or incursion of relatively warm water into subshelf ocean cavities. The resulting melting, weakening, and potential ice-shelf collapse reduces shelf buttressing effects. Upstream ice flow accelerates, causing thinning, grounding-line retreat, and potential ice sheet collapse. While high-resolution projections have been performed for localized Antarctic regions, full-continent simulations have typically been limited to low-resolution models. Here we quantify the vulnerability of the entire present-day AIS to regional ice-shelf collapse on millennial timescales treating relevant ice flow dynamics at the necessary ~1km resolution. Collapse of any of the ice shelves dynamically connected to the West Antarctic Ice Sheet (WAIS) is sufficient to trigger ice sheet collapse in marine-grounded portions of the WAIS. Vulnerability elsewhere appears limited to localized responses.

1 Introduction

The contribution of the Antarctic Ice Sheet (AIS) remains the largest source of uncertainty in projections of future sea level rise (SLR) [*Church et al.*, 2013]. The flow of ice from the Antarctic interior to the sea is organized into networks of relatively fast-flowing (1-10 km/year) ice streams, which flow over submarine bedrock to feed large floating ice shelves (fig 1). The boundary between *grounded* ice (ice thick enough to rest on submarine bedrock) and floating ice is known as the *grounding line* (GL), and it is this transitional region that must be treated with care in models of the AIS. [*Durand et al.*, 2009; *Cornford et al.*, 2016; *Pattyn et al.*, 2013]. Finally, ice enters the ocean either via basal melting (due to the presence of relatively warm and saline ocean water reaching the underside of floating ice), surface melting (via hydrofracture-driven crevasses), or through iceberg calving. In turn, ice shelves affect their feeder ice streams through a "buttressing" effect [*Asay-Davis et al.*, 2016; *Gudmundsson*, 2013; *Goldberg et al.*, 2009], slowing them and reducing their discharge. Ice shelf thinning and collapse lead to reduction or elimination of this buttressing effect, leading in turn to acceleration, thinning, and retreat of the ice sheet, particularly via the Marine Ice Sheet Instability [*Weertman*, 1974; *Schoof*, 2007]. This has been both inferred from observations [*Rignot et al.*, 2014] and demonstrated by modelling [*Favier et al.*, 2014]. *Fürst et al.* [2016] evaluated the buttressing effect in Antarctic ice shelves based on an analysis of their instantaneous stress state, which provides an indication of the short-term dynamic consequences of ice shelf collapse, but leaves open the question of the larger, longer-term effects once retreat has begun. How this retreat progresses will be dominated by effects like the Marine Ice Sheet Instability, which is dependent on the topography underlying the ice sheet. [*Weertman*, 1974; *Schoof*, 2007]

While high resolution projections have been performed for localized Antarctic regions like the Pine Island and Thwaites glaciers [*Favier et al.*, 2014; *Waibel et al.*, 2018], simulations of the whole continent have typically been limited to low resolution models. However, in recent years the accuracy of such projections from low-resolution models has been called into question. [*Durand et al.*, 2009; *Cornford et al.*, 2016; *Pattyn et al.*, 2013; *Reese et al.*, 2018]. Here, we use the BISICLES ice sheet model [*Cornford et al.*, 2015], which deploys sub-kilometer mesh resolution in key zones, to simulate the response of the entire continental ice sheet to regional ice shelf collapse. Such fine resolution has been demonstrated to be necessary for the correct representation of the stresses at the grounding line, to the extent that numerical error can otherwise overshadow projections of AIS mass budget and stability [*Durand et al.*, 2009; *Cornford et al.*, 2016, 2013; *Pattyn et al.*, 2013; *Reese et al.*, 2018]. BISICLES achieves this fine resolution through adaptive mesh refinement, dynamically deploying computationally-expensive fine resolution only when and where needed to accurately resolve the evolving dynamics of the ice sheet.

Subjecting each and every ice shelf to extreme thinning, such that any floating ice is reduced to a thickness of 100m within a few years of its detachment from the bed, leads to the complete collapse of the West Antarctic Ice Sheet and pronounced retreat in several East Antarctic basins, amounting to 4.6 m sea level rise over 500 years [*Cornford et al.*, 2016]. While this is an unrealistically high thinning rate, it does represent an upper bound on the rate of sea level rise due to continent-wide ice shelf thinning; by extension, it is natural to estimate the upper bound on the ice sheet's vulnerability to *regional* ice shelf collapse by, for example, confining such forcing to the Amundsen Sea Embayment, where ocean-induced retreat has already been observed [*Rignot et al.*, 2014]. We divided Antarctica into 14 sectors (Figure 1), corresponding to a broad-scale map of Antarctic ice drainage basins similar to that in *Zwally et al.* [2012]. For each sector, we ran an experiment in which we applied extreme ice-shelf thinning to any floating ice in the sector, evolving the ice sheet for 1000 years. Simulations with coupled ice-sheet and ocean models [*Asay-Davis et al.*, 2016] suggest that subshelf melt forcing will follow grounding lines as they retreat. Thus, melt forcing is allowed to follow grounding lines as they retreat into the interior of the continent, even out of the original sector. To test whether melt following the grounding line over such large-scale retreat was essential, we ran a second set of experiments in which this thinning was confined to the chosen sector. In some cases, grounding lines retreated out of the selected sector, at which point the forcing stopped and any further retreat was unforced. While our experiments implemented ice shelf weakening specifically due to submarine melting, surface melting like that seen on the Siple Coast in 2016 [*Nicolas et al.*, 2017] can also result in weakening and eventual collapse of ice shelves, as observed in the Larsen B Ice Shelf breakup in 2002 [*van den Broeke*, 2005; *McGrath et al.*, 2012]. The effects of ice shelf loss in this work are independent of the specific form of shelf weakening; rather, they indicate the general vulnerability of the AIS to the weakening and loss of its floating ice shelves.

2 Methods

We began with the Antarctic "present-day" initial condition used in *Cornford et al.* [2016], which is based on the Bedmap2 dataset [*Fretwell et al.*, 2013]. We use the present-day temperature field computed by *Pattyn* [2010], and the accumulation field from *Arthern et al.* [2006]. Using the Antarctic sector map (1) as a mask, we applied the extreme melting scenario from *Cornford et al.* [2016] to any floating ice in the chosen sector(s) and then evolved the ice sheet in each melt configuration for 1000 years using the BISICLES ice sheet model [*Cornford et al.*, 2013]. The adaptive mesh refinement (AMR) capabilities of the BISICLES model enabled us to apply sufficiently fine spatial and temporal resolution (as demonstrated in *Cornford et al.* [2016]) to accurately resolve the grounding line dynamics of the ice sheet. The finest resolution (1km) was applied near grounding lines, dynamically adapting the resolution and following the grounding lines as the solution evolved. This resolution, when coupled with a subgrid-friction scheme, has been demonstrated to be sufficient for this experiment in *Cornford et al.* [2016] and in the supplementary material. The submarine melt forcing used in this work is depth-dependent, ranging from no melting for ice shelves with a thickness less than 100m, then linearly increasing with ice shelf draft up to a maximum ablation value of 400 meters/year (m/a) where the ice thickness is greater than 800m.[1] While this produces unrealistically high melt rates, the intent is to test the ice sheet's sensitivity to forcing, not produce credible temporally-accurate projections (which will be left to a following work). Limiting thinning to shelves with greater than 100m thickness rather than thinning all the way to zero thickness is a numerical convenience. The supplementary material includes a demonstration that the 100m cutoff is thin enough to be dynamically similar to thinning all the way to zero, while avoiding a set of numerical difficulties which occasionally occur when portions

[1] There is an error in the forcing function specified in *Cornford et al.* [2016] – the values here are the correct ones.

of ice shelves are removed entirely. As recommended in *Seroussi and Morlighem* [2018], we confine melting to computational cells which are fully floating.

We performed two sets of experiments. In the first, the melt forcing associated with a given sector or sectors was allowed to follow the grounding line retreat anywhere within that sector or more than 100km distant from the initial ice shelf region of another sector. In the second set, subshelf melt forcing was confined to the chosen sector or sectors. In a few cases (particularly sector 5), grounding lines passed out of the sector, at which point the melt forcing would no longer follow the grounding line retreat (but grounding lines were free to continue their retreat, and did). We also ran a control experiment with no subshelf melting, which showed a tendency to gain ice after about 100 years, gaining 197mm SLE after 500 years and 467 mm SLE after 1000 years, primarily due to accumulation in the interior. While this control does not take present-day retreat and subshelf melting rates into account, the goal of this work is to evaluate vulnerability to *any* shelf weakening and collapse, including any which may already underway, while the tendency of the control to add ice tends to isolate just the response due to the applied forcing, while not affecting the dynamics of the response. To isolate the effect of the melt-induced dynamics, we subtracted the control solution from the results of the runs. We then evaluated the change in the volume of ice over flotation (VoF), the net contribution to global sea levels.

While our experiment design aims to capture the important ice physics relevant to the dynamics of marine ice sheet instability, certain processes are not incorporated in our model. In this work, we do not incorporate the marine ice cliff instability proposed in [*Pollard et al.*, 2015] and [*DeConto and Pollard*, 2016], which remains controversial and has not been fully developed in a modeling context. Also, while we incorporate a realistic ice temperature field in our initial condition, we do not evolve that temperature field as the experiments progress. We believe this to be a reasonable approximation for much of this experiment given the rapid nature of the response compared to the relatively slow timescale of thermal evolution in the ice. At the same time, it is likely that this omission results in generally colder ice than would result from fully thermomechanically-coupled simulations, and so would tend to *underestimate* ice sheet response. Similarly, the basal friction field we compute to match our initial velocity field to observations remains fixed for the duration of the runs. While this is also not realistic, we expect it will primarily miss the tendency of bed friction to reduce as the grounding lines move inland and ice flow becomes more active, which will also tend to under-predict acceleration, thinning, and retreat in the ice sheet.

Plots of ice thickness differences relative to the control and plots of contribution to sea level rise vs. time for each case are provided in the supplementary materials.

3 Results

Figure 2 shows the contribution to SLR after 1000 years due to shelf loss for each sector, compared to the control, which had no thinning, along with the result from forcing all sectors simultaneously, which resulted in a response of 4.6m of eustatic sea level equivalent (SLE) after 1000 years. In all cases, regional ice shelf collapse caused at least some enhanced Antarctic contribution to SLR when compared to the control. We observe three tiers of response. The first tier, comprising the largest responses, includes sectors 2 (the Amundsen Sea Embayment), 4 (the portion of the Ross Ice Shelf adjacent to Siple Coast streams), and 5 (the western part of the Ronne Ice Shelf) with or without out-of-sector melting, and sector 14 (the portion of the Ross ice shelf adjacent to the Transantarctic Mountains) if out-of-sector melting is permitted, range from 2.2 to 2.6 m of SLE, and come from retreat chronologies in which grounding-line retreat reaches the interior of the West Antarctic Ice Sheet (WAIS), as illustrated in Figure 3. The striking feature of these results is that all four high-impact cases trigger continental scale retreat in the same vulnerable submarine-grounded part of WAIS, but through different routes. As shown in Figure 3, forcing from Sector 2 drains ice through the Thwaites Glacier basin into the Amundsen Sea, forcing from sector 5 drains ice through the Rutford Ice Stream into the Ronne Ice Shelf and ultimately the Weddell Sea, and forcing from Sectors 4 and 14 drains into the Ross Sea. This result indicates the high degree of vulnerability of the marine-grounded portions of the WAIS to the weakening of any of its dynamically-connected ice shelves and agree generally with *Feldmann and Levermann* [2015a], in which a similar study was conducted for a regional WAIS domain forced from the Amundsen Sea. Notably, sector 14 only has limited access to the vulnerable part of WAIS via the Whillans and Mercer ice streams, but depending on the evolution of shelf collapse as those grounding lines retreat, thinning in that sector can cause WAIS collapse similar to the more well-connected (to the WAIS interior) sectors. At the same time, its limited impact when melting remains in-sector underscores the difference between the level of vulnerability in the EAIS and WAIS. This also highlights the nature of the Siple Coast as an effective route to WAIS collapse, which has yet to be extensively studied by current models. On the other hand, the limited-melt experiment results for sectors 2, 4, and 5 indicate a high degree of vulnerability of the WAIS even to unforced retreat once retreating grounding lines breach the boundaries of the region, with much of the retreat and loss in the central WAIS occurring out of the originally-forced sector.

The second tier of AIS response consists of ice streams whose cumulative contribution to SLR is comparable to the main WAIS system and is evident in Figure 2. Forcing applied to sectors 6 (including the Support Force and Foundation glaciers), 7 (the Bailey, Slessor, and Recovery ice streams flowing into the Filchner Ice Shelf), and 13 (George V land, including the Wilkes sub-glacial basin) results in 300 – 600 mm SLE in each case, as it does in sector 14 if melting does not progress beyond the sector (Figures S3, S4, and S7 in the supplementary material). In all of these cases, only minimal effects are seen outside the immediately affected drainage basins.

The third tier comprises the remaining 7 sectors, which each exhibit millennial ice losses of less than 200 mm SLE. A notable case is that of the Totten and Vanderford glaciers (in sector 12, Wilkes Land), which undergo rapid retreat at the start of the simulations but for which the relatively limited mass loss is ultimately restricted to the deep trough surrounding Law Dome. This suggests that the current activity observed in this sector [*Rintoul et al.*, 2016; *Xin et al.*, 2015] is not likely to result in large contributions to SLR in the long term.

Even with the extreme forcing employed in this experiment, most of the contribution to sea level rise occurs well after the first 100 years. The initial loss comprises small contributions from every sector of the ice sheet (all the way around the margin), whereas the the potential for larger, longer-term loss is dominated by the sectors which activate WAIS collapse.

Regional Independence

Due to limitations in computational resources, it is currently common practice to model individual AIS drainage basin evolution separately. For example, previous studies have examined the response of the Pine Island Glacier [*Favier et al.*, 2014; *Cornford et al.*, 2013], the Thwaites Glacier [*Waibel et al.*, 2018; *Seroussi et al.*, 2017; *Joughin et al.*, 2014], or multiple glaciers in the same catchment [*Cornford et al.*, 2015]. On the other hand, studies which examine the entire AIS have tended to employ low spatial resolution and/or parameterized critical dynamical processes due to the prohibitive computational expense of modeling the entire ice sheet at high resolutions [*DeConto and Pollard*, 2016; *Winkelmann et al.*, 2015; *Golledge et al.*, 2015]. The validity of sea level projections based on regional simulations depends on the assumption of independence of the region in question from ice dynamics occurring elsewhere in the ice sheet, which may have question-

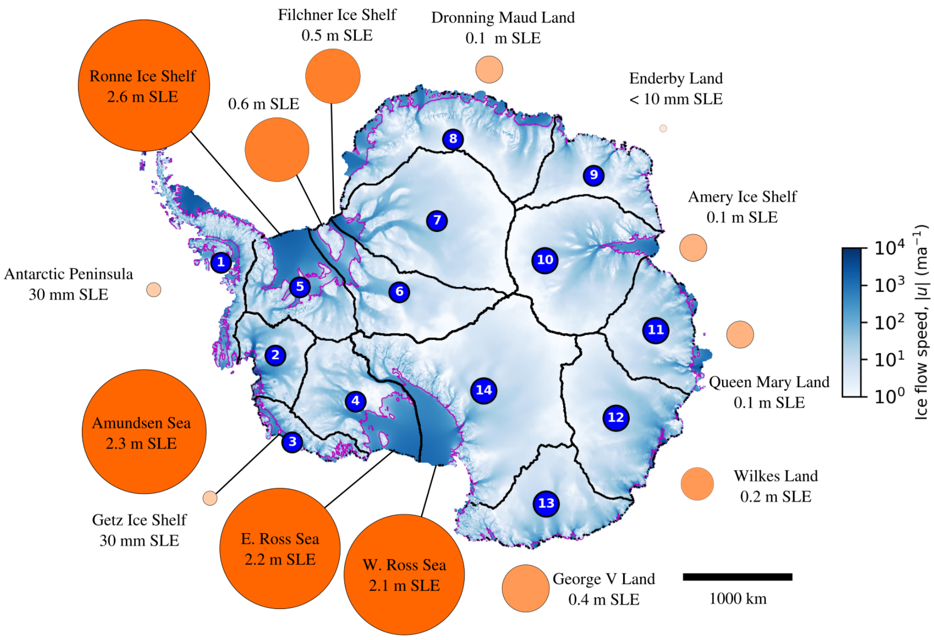

Figure 1. Antarctic vulnerability to localized ice shelf collapse. Initial modeled flow speed is shown in shaded blue. Magenta lines indicate initial grounding-line locations. Mass lost above flotation (eustatic sea level equivalent, SLE) after 1000 years of extreme, sustained ice shelf thinning originating in the numbered sectors is illustrated by the adjacent circle area.

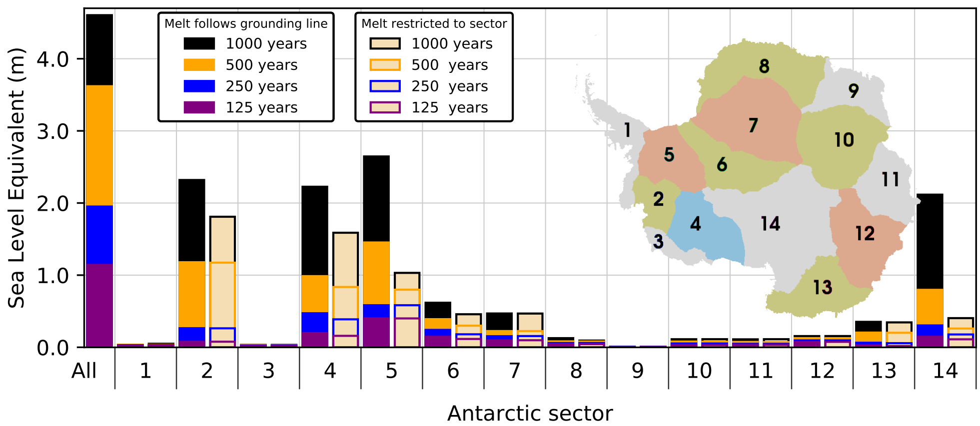

Figure 2. 1000-year contribution to sea level rise (in mm SLE) after 125,250, 500, and 1000 years for each Antarctic sector. Results from both experiments are shown; for each sector, the left bar shows the case where melt is restricted to the specified sector and the right bar shows the case where melt is allowed to follow grounding lines into other sectors. "All" is the case where there is melting in all sectors simultaneously.

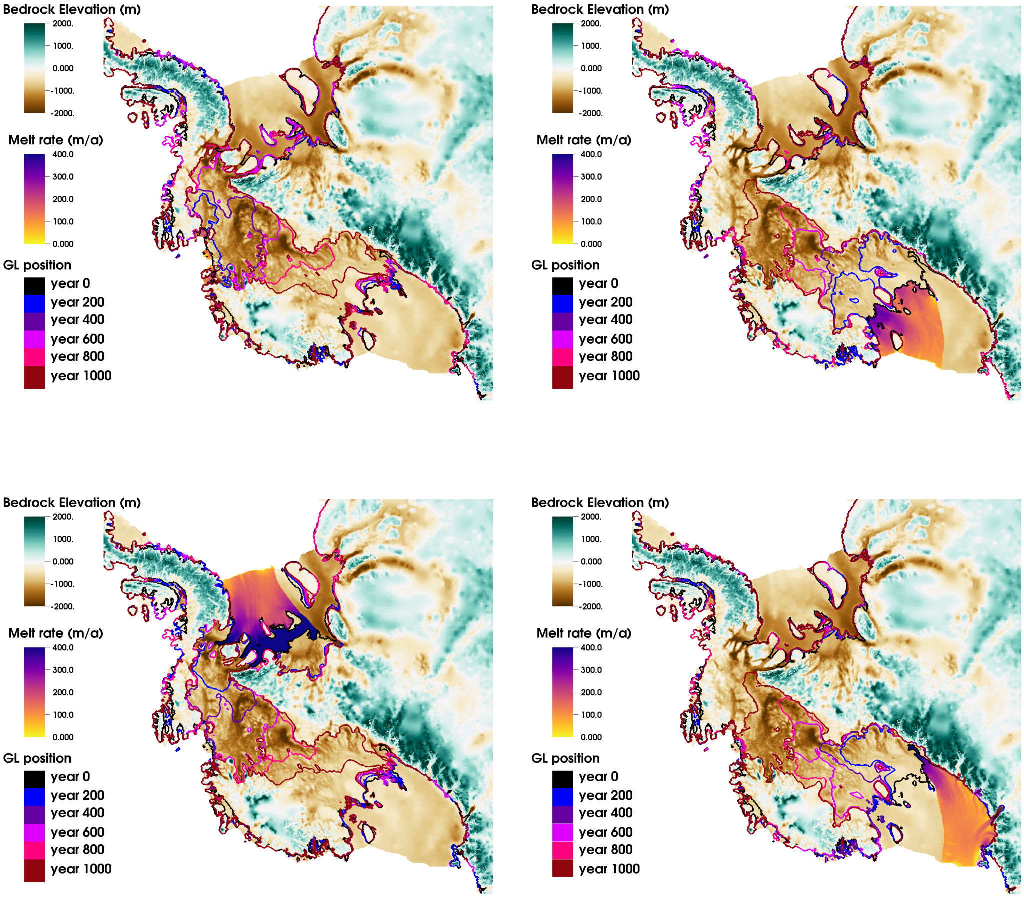

Figure 3. Grounding-line evolution illustrated with contours every 200 years for sectors 2 (upper left), 4 (upper right), 5 (lower left), and 14 (lower right). Colormap shows initial melt-forcing distribution for each case.

able validity given the multiple vulnerabilities of the WAIS shown above. This type of inter-basin interaction was examined in an idealized setting in *Feldmann and Levermann* [2015b]. To test this in the Antarctic setting, we also subjected selected combinations of sectors to simultaneous melt forcing to determine whether different connected sectors of the WAIS truly evolve independently. We examine two configurations. In the first, we examine the regional independence of the first-tier sectors which directly drive WAIS collapse. In particular, we examine the combinations of sectors 2&4 and 2&5. The third possible combination, 4&5, is less relevant due to the current active retreat in the ASE region (sector 2), but is included in the supplemental materials for completeness. The second configuration examines the independence of different parts of the large ice shelves (i.e. the combinations of sectors 5&6 and 4&14). Time-dependent plots of the volume above flotation (VaF) (i.e. the contribution to SLR) are shown in figure 4 while the rate of change of VaF (rate of contribution to SLR) is shown in figure 5. If ice dynamics for each sector are independent, then the results of the combined run (purple lines in figures 4 and 5) and the sum of the individual runs (green lines in figures 4 and 5) should be identical. As seen in Figure 4, this generally holds true in WAIS-connected sectors for about 100 years, after which the assumption of regional independence appears to break down somewhat as small differences appear. The differences remain small for a further 300-400 years time, at which point grounding lines retreat significantly out of their original drainage basins and the independent runs begin to contend for the same grounded ice, and so can no longer be treated additively.

The exception to this is for the Ronne Ice shelf sectors, (figure 4, lower left) where WAIS collapse is entirely due to forcing in the western part of sector 5 but the most dramatic, near-future retreat, associated with the Möller and Institute ice streams, is hastened by the inclusion of forcing in the eastern part of sector 6.

In general, distinguishable "events" in the plots in figure 5 – such as WAIS collapse when rates of SLR grow to 5 $\mathrm{mm\,a^{-1}}$ – occur earlier when both sectors are forced, suggesting that temporally-detailed projections of sea level contributions for time scales longer than centennial may require the use of whole-continent (or at least whole-WAIS/EAIS) models. It is, however, also possible that realistic forcing scenarios will preserve dynamic independence (and thus the validity of regional modeling) longer, given the extreme nature of the applied forcing in this set of experiments.

4 Discussion and Conclusions

In summary, we find that the primary Antarctic vulnerability to submarine melting and shelf collapse remains the collapse of the West Antarctic Ice Sheet. There are three primary routes to WAIS collapse. Beyond the currently-active vulnerability to retreat in the Amundsen Sea Sector, we also find that the WAIS is vulnerable to weakening or collapse of the Ronne Ice Shelf via the Rutford Ice Stream, as well as a broader vulnerability via the ice streams of the Siple Coast. The remaining vulnerabilities, particularly in the East Antarctic Ice Sheet, are much smaller and are regionally contained. This tends to confirm earlier studies performed with coarse-grid, heavily parameterized models. While this work clarifies the vulnerability of the Antarctic Ice Sheet, placing what is likely an upper bound on its response to local incursions of circumpolar deep water (CDW) or surface-melt-driven hydrofracture, it falls to global circulation models and ocean models (especially those with active ice-ocean coupling) to quantify the likelihood and timing of such shelf-collapse forcing (such as the warm-water incursion predicted by *Hellmer et al.* [2017] for the Weddell Sea ice shelves), and the potential coupling with shelf weakening due to surface-melt driven hydrofracture. We also find that, at least for the cases examined in this work, regional ice sheet models are likely sufficient for these projections for 400-500 years for broadly characterizing ice sheet response, but whole ice-sheet models may be required for time-accurate projections beyond the century scale.

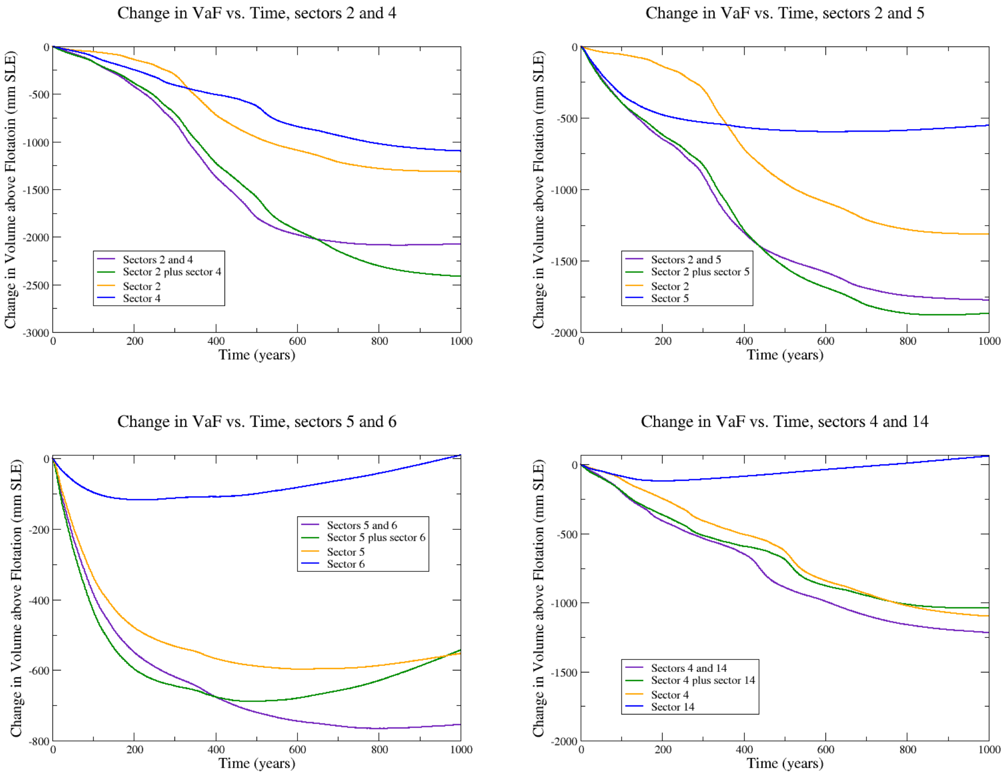

Figure 4. Change in Volume above Flotation (in mm Sea Level Equivalent (SLE)) for selected combinations of sectors: (top left) Sectors 2 & 4, (top right) sectors 2 & 5, (bottom left) sectors 5 & 6, and (bottom right) sectors 4 & 14. In each plot, the purple line is the case with both sectors forced simultaneously, green is the sum of the two independently forced values, and the orange and blue lines represent the individual sectors.

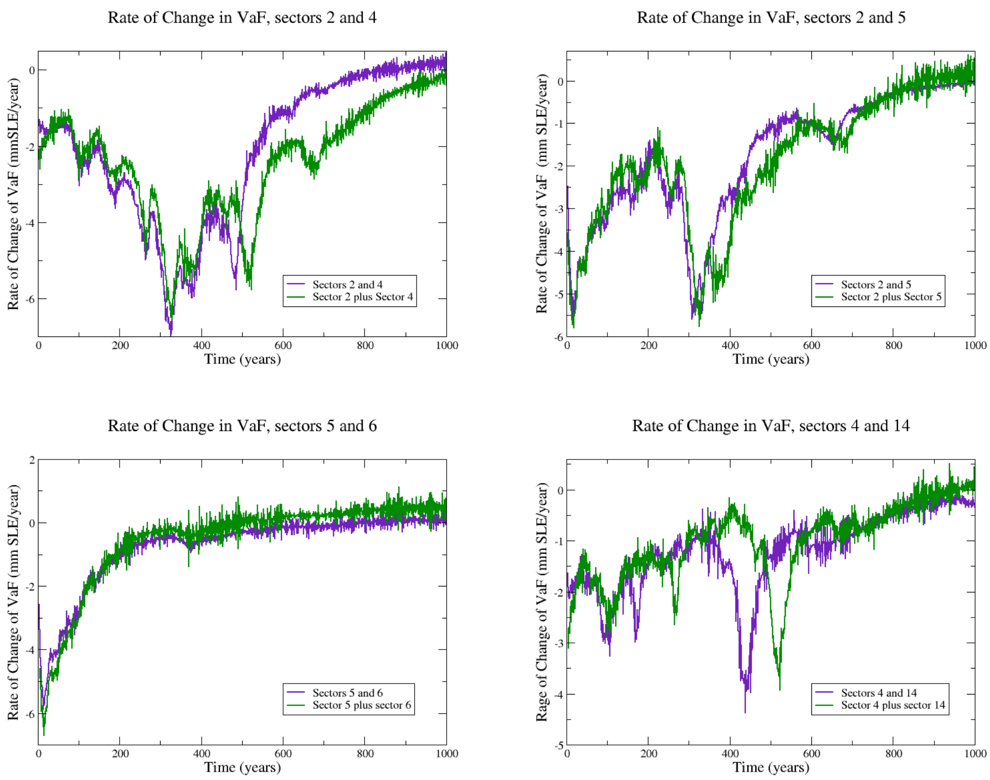

Figure 5. Rate of change in Volume above Flotation (in mm Sea Level Equivalent (SLE)) for selected combinations of sectors: (top left) Sectors 2 & 4, (top right) sectors 2 & 5, (bottom left) sectors 5 & 6, and (bottom right) sectors 4 & 14. Purple is both sectors simultaneously, and green is the sum of the two independently-run values.

Citations

Acknowledgments

The authors gratefully acknowledge input from Stephen Price, Matthew Hoffman, and Esmond Ng. We also thank the two anonymous reviewers, whose thoughtful suggestions improved this work. Work at LBL was supported by the Director, Office of Science, Offices of Advanced Scientific Computing Research (ASCR) and Biological and Environmental Research (BER), of the U.S. Department of Energy under Contract No. DE-AC02-05CH11231, as a part of the ProSPect SciDAC Partnership. This research used resources of the National Energy Research Scientific Computing Center, a DOE Office of Science User Facility supported by the Office of Science of the U.S. Department of Energy under Contract No. DE-AC02-05CH11231.

Code and data availability.

We used the publicly-available version of the BISICLES ice sheet model code, release version 1.0. Instructions for downloading and installing BISICLES may be found in the "getting started" section at `http://bisicles.lbl.gov`. BISICLES is written in a combination of C++ and FORTRAN, and is built upon the Chombo AMR software framework. More information about Chombo may be found at `http://Chombo.lbl.gov`.

Data, input , and configuration files for the runs in this work are available at:
`http://portal.nersc.gov/project/iceocean/AntarcticRegionalMelt/`

References

Arthern, R. J., D. P. Winebrenner, and D. G. Vaughan (2006), Antarctic snow accumulation mapped using polarization of 4.3-cm wavelength microwave emission, *Journal of Geophysical Research: Atmospheres*, *111*(D6), n/a–n/a, doi:10.1029/2004JD005667.

Asay-Davis, X. S., S. L. Cornford, G. Durand, B. K. Galton-Fenzi, R. M. Gladstone, G. H. Gudmundsson, T. Hattermann, D. M. Holland, D. Holland, P. R. Holland, D. F. Martin, P. Mathiot, F. Pattyn, and H. Seroussi (2016), Experimental design for three interrelated marine ice sheet and ocean model intercomparison projects: MISMIP v. 3 (MISMIP+), ISOMIP v. 2 (ISOMIP+) and MISOMIP v. 1 (MISOMIP1), *Geosci. Model Dev.*, *9*(7), 2471–2497, doi:10.5194/gmd-9-2471-2016.

Church, J., P. Clark, A. Cazenave, J. Gregory, S. Jevrejeva, A. Levermann, M. Merrifield, G. Milne, R. Nerem, P. Nunn, A. Payne, W. Pfeffer, D. Stammer, and A. Unnikrishnan (2013), *Sea Level Change*, book section 13, pp. 1137–1216, Cambridge University Press, Cambridge, United Kingdom and New York, NY, USA, doi: 10.1017/CBO9781107415324.026.

Cornford, S. L., D. F. Martin, D. T. Graves, D. F. Ranken, A. M. Le Brocq, R. M. Gladstone, A. J. Payne, E. G. Ng, and W. H. Lipscomb (2013), Adaptive mesh, finite volume modeling of marine ice sheets, *Journal of Computational Physics*, *232*(1), 529–549.

Cornford, S. L., D. F. Martin, A. J. Payne, E. G. Ng, A. Le Brocq, R. M. Gladstone, T. L. Edwards, S. R. Shannon, C. Agosta, M. R. Van Den Broeke, H. H. Hellmer, G. Krinner, S. R. M. Ligtenberg, R. Timmermann, and D. G. Vaughan (2015), Century-scale simulations of the response of the West Antarctic Ice Sheet to a warming climate, *The Cryosphere*, *9*(4), 1579–1600.

Cornford, S. L., D. F. Martin, V. Lee, A. J. Payne, and E. G. Ng (2016), Adaptive mesh refinement versus subgrid friction interpolation in simulations of Antarctic ice dynamics, *Annals of Glaciology*, *57*(73), doi:10.1017/aog.2016.13.

DeConto, R. M., and D. Pollard (2016), Contribution of Antarctica to past and future sea-level rise, *Nature*, *531*, 591–597, doi:10.1038/nature17145.

Durand, G., O. Gagliardini, T. Zwinger, E. L. Meur, and R. C. Hindmarsh (2009), Full Stokes modeling of marine ice sheets: influence of the grid size, *Annals of Glaciology*, *50*(52), 109–114, doi:10.3189/172756409789624283.

Favier, L., G. Durand, S. L. Cornford, G. H. Gudmundsson, O. Gagliardini, F. Gillet-Chaulet, T. Zwinger, A. J. Payne, and A. M. Le Brocq (2014), Retreat of Pine Island Glacier controlled by marine ice-sheet instability, *Nature Climate Change*, *5*(2), 1–5, doi:10.1038/nclimate2094.

Feldmann, J., and A. Levermann (2015a), Collapse of the West Antarctic Ice sheet after local destabilization of the Amundsen Basin, *112*(46), 14,191–14,196, doi:10.1073/pnas.1512482112.

Feldmann, J., and A. Levermann (2015b), Interaction of marine ice-sheet instabilities in two drainage basins: simple scaling of geometry and transition time, *The Cryosphere*, *9*(2), 631–645, doi:10.5194/tc-9-631-2015.

Fretwell, P., H. D. Pritchard, and D. G. Vaughan (2013), Bedmap2: improved ice bed, surface and thickness datasets for Antarctica, *Cryosph.*, *7*(1), 375–393, doi:10.5194/tc-7-375-2013.

Fürst, J. J., G. Durand, F. Gillet-Chaulet, L. Tavard, M. Rankl, M. Braun, and O. Gagliardini (2016), The safety band of Antarctic ice shelves, *Nature Climate Change*, *6*(5), 479–482.

Goldberg, D., D. M. Holland, and C. Schoof (2009), Grounding line movement and ice shelf buttressing in marine ice sheets, *Journal of Geophysical Research*, doi:10.1029/2008JF001227.

Golledge, N. R., D. E. Kowalewski, T. R. Naish, R. H. Levy, C. J. Fogwill, and E. G. W. Gasson (2015), The multi-millennial Antarctic commitment to future sea-level rise, *Nature*, *526*(7573), 421–425.

Gudmundsson, G. H. (2013), Ice-shelf buttressing and the stability of marine ice sheets, *The Cryosphere*, *7*(2), 647–655, doi:10.5194/tc-7-647-2013.

Hellmer, H., F. Kauker, R. Timmermann, and T. Hattermann (2017), The fate of the Southern Weddell Sea continental shelf in a warming climate, *J. Climate*, *30*, 4337âĂŞ4350, doi:https://doi.org/10.1175/JCLI-D-16-0420.1.

Joughin, I., B. E. Smith, and B. Medley (2014), Marine Ice Sheet Collapse Potentially Under Way for the Thwaites Glacier Basin, West Antarctica, *Science*, *344*(6185), 735–738.

McGrath, D., K. Steffen, H. Rajaram, T. Scambos, W. Abdalati, and E. Rignot (2012), Basal crevasses on the Larsen C Ice Shelf, Antarctica: Implications for meltwater ponding and hydrofracture, *Geophysical Research Letters*, *39*(16), doi:10.1029/2012GL052413, l16504.

Nicolas, J. P., A. M. Vogelmann, R. C. Scott, A. B. Wilson, M. P. Cadeddu, D. H. Bromwich, J. Verlinde, D. Lubin, L. M. Russell, C. Jenkinson, H. H. Powers, M. Ryczek, G. Stone, and J. D. Wille (2017), January 2016 extensive summer melt in West Antarctica favoured by strong El Niño, *Nature Communications*, *8*, doi:doi:10.1038/ncomms15799.

Pattyn, F. (2010), Antarctic subglacial conditions inferred from a hybrid ice sheet/ice stream model, *Earth and Planetary Science Letters*, *295*(3), 451 – 461, doi:https://doi.org/10.1016/j.epsl.2010.04.025.

Pattyn, F., L. Perichon, G. Durand, L. Favier, O. Gagliardini, R. C. Hindmarsh, T. Zwinger, T. Albrecht, S. Cornford, D. Docquier, and et al. (2013), Grounding-line migration in plan-view marine ice-sheet models: results of the ice2sea MISMIP3d intercomparison, *Journal of Glaciology*, *59*(215), 410–422, doi:10.3189/2013JoG12J129.

Pollard, D., R. M. DeConto, and R. B. Alley (2015), Potential Antarctic Ice Sheet retreat driven by hydrofracturing and ice cliff failure, *Earth and Planetary Science Letters*, *412*, 112 – 121, doi:https://doi.org/10.1016/j.epsl.2014.12.035.

Reese, R., R. Winkelmann, and G. H. Gudmundsson (2018), Grounding-line flux formula applied as a flux condition in numerical simulations fails for buttressed Antarctic ice streams, *The Cryosphere Discussions*, *2018*, 1–22, doi:10.5194/tc-2017-289.

Rignot, E., J. Mouginot, M. Morlighem, H. Seroussi, and B. Scheuchl (2014), Widespread, rapid grounding line retreat of Pine Island, Thwaites, Smith, and Kohler glaciers, West Antarctica, from 1992 to 2011, *Geophysical Research Letters*, *41*(10), 3502–3509.

Rintoul, S. R., A. Silvano, B. Pena-Molino, E. van Wijk, M. Rosenberg, J. S. Greenbaum, and D. D. Blankenship (2016), Ocean heat drives rapid basal melt of the Totten Ice Shelf, *Science Advances*, *2*(12), doi:10.1126/sciadv.1601610.

Schoof, C. (2007), Ice sheet grounding line dynamics: Steady states, stability, and hysteresis, *Journal of Geophysical Research-Earth Surface*, *112*(F3).

Seroussi, H., and M. Morlighem (2018), Representation of basal melting at the grounding line in ice flow models, *The Cryosphere*, *12*(10), 3085–3096, doi:10.5194/tc-12-3085-2018.

Seroussi, H., Y. Nakayama, E. Larour, D. Menemenlis, M. Morlighem, E. Rignot, and A. Khazendar (2017), Continued retreat of Thwaites Glacier, West Antarctica, controlled by bed topography and ocean circulation, *Geophysical Research Letters*, *44*(12), 6191–6199, doi:10.1002/2017GL072910.

van den Broeke, M. (2005), Strong surface melting preceded collapse of Antarctic Peninsula ice shelf, *Geophysical Research Letters*, *32*(12), doi:10.1029/2005GL023247, l12815.

Waibel, M. S., C. L. Hulbe, C. S. Jackson, and D. F. Martin (2018), Rate of mass loss across the instability threshold for Thwaites Glacier determines rate of mass loss for entire basin, *Geophysical Research Letters*, *45*(2), 809–816, doi:10.1002/2017GL076470.

Weertman, J. (1974), Stability of the junction of an ice sheet and an ice shelf, *Journal of Glaciology*, *13*, 3–13.

Winkelmann, R., A. Levermann, A. Ridgwell, and K. Caldeira (2015), Combustion of available fossil fuel resources sufficient to eliminate the Antarctic Ice Sheet, *Science Advances*, *1*(8), e1500,589–e1500,589.

Xin, L., R. Eric, M. Mathieu, M. Jeremie, and S. Bernd (2015), Grounding line retreat of Totten Glacier, East Antarctica, 1996 to 2013, *Geophysical Research Letters*, *42*(19), 8049–8056, doi:10.1002/2015GL065701.

Zwally, H., M. Giovinetto, M. A. Beckley, and J. Saba (2012), Antarctic and Greenland drainage systems, *Tech. rep.*